[Original paper]
Journal of the Korean Society for Nondestructive Testing
Vol. 32, No. 2 (2012. 4)

Non-Destructive Evaluation of Material Properties of Nanoscale Thin-Films Using Ultrafast Optical Pump-Probe Methods

Yun Young Kim* and Sridhar Krishnaswamy*†

Abstract Exploration in microelectromechanical systems(MEMS) and nanotechnology requires evaluation techniques suitable for sub-micron length scale so that thermal and mechanical properties of novel materials can be investigated for optimal design of miro/nanostructures. The ultrafast optical pump-probe technique provides a contact-free and non-destructive way to characterize nanoscale thin-films, and its ultrahigh temporal resolution enables the study of heat-transport phenomena down to a sub-picosecond regime. This paper reviews the principle of optical pump-probe technique and introduces its application to the area of micro/nano-NDE.

Keywords: Picosecond Ultrasonics, Laser-Based Non-Destructive Evaluation, Thin-Film, Materials Characterization

1. Introduction

Nanoscale thin-film materials and structures are a subject of active research today because of their wide-ranging applications in science and engineering. Carbon-based materials such as graphene or diamond-like carbon(DLC) exist in a 2-dimensional form, and MEMS devices such as radio-frequency(RF) switches or microcantilevers are made of membranes or metallic layers.

In order to optimize the device performance and prevent structural failure, it is important to understand the thermal and mechanical properties of thin-film materials. They are, however, not necessarily identical to those of bulk materials due to scale effects and large surface-area-to-volume ratio[1]. Besides, the properties could vary depending on the fabrication technique even for the same material[2]. For these reasons, investigations have been performed to develop a characterization technique for MEMS and nano-materials/structures. There are many methods such as nanoindentation[3], mirage technique[4], bulge testing[5], 3ω method[6], and so on.

Unlike these methods, however, the optical pump-probe technique provides a non-contact and non-destructive way to characterize nanomaterials with very high temporal resolution down to sub-picosecond. In this technique, ultrafast laser pulses are focused onto the surface of a metal-coated sample so that the optical energy can be absorbed. The resulting expansion and cooling of the local spot on the film surface results in temperature-induced reflectivity changes as well as generation of high-frequency ultrasonic waves propagating in the thin film. If the sample is composed of two or more layers, the film interface will produce echoes of ultrasound, and as a result additional changes of surface reflectivity will be observed when the echo arrives due to the piezo-optic effect. These changes are monitored through the intensity change of a probe laser beam, which is illuminated on the same spot and reflected to a photodetector. Fig. 1 schematically describes the principle. Analysis of the plot provides thermal

[Received: February 24, 2012, Revised: April 11, 2012, Accepted: April 13, 2012] *Department of Mechanical Engineering, Northwestern University, Evanston IL 60208, USA †Corresponding Author: s-krishnaswamy@northwestern.edu

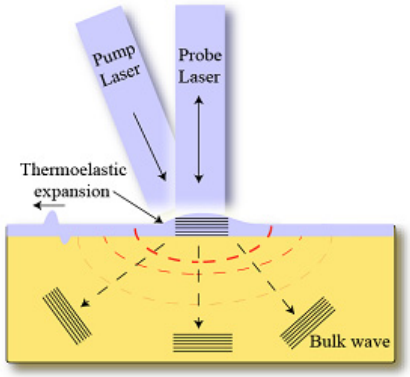

Fig. 1 The principle of picosecond ultrasonics[8]

and mechanical properties of nanoscale materials such as thermal conductivity, film thickness, sound velocity, Young's modulus, interfacial adhesion quality, sub-surface morphology, and so on[7].

Therefore, the technique has become very popular in the area of thin-film and nanomaterials research today. In this review paper, the principle of ultrafast pump-probe technique will be discussed, and its applications in the area of micro/nano NDE will be introduced.

2. Experimental

2.1 Optics Setup

Fig. 2 describes the schematic of a standard optical pump-probe setup. A femtosecond laser system emits a train of pulses, and commercially available lasers nowadays typically have parameters of ~100 fs pulse width, 780~800 nm wavelength, 80 MHz repetition rate, and 8~34 nJ pulse energy. With a combination of half-wave plate and polarizing beam splitter, the beam is divided into pump- and probe-paths with an intensity ratio of 10:1. Here, the pump-beam is chopped using an acousto- or electro-optic modulator to provide a reference frequency to a lock-in amplifier and focused onto the sample surface to induce periodic

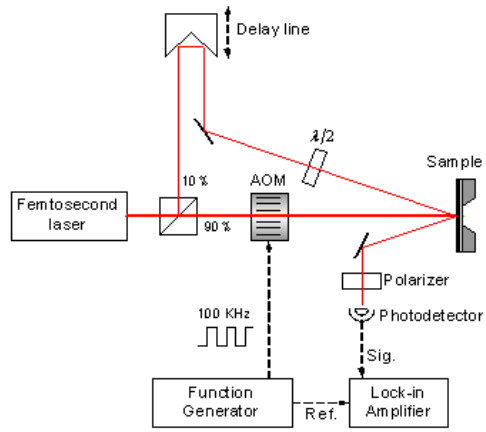

Fig. 2 A schematic of the experimental setup

temperature rise and decay. Meanwhile, the probe-beam is directed and focused to the same spot where the pump-beam falls using a retroreflector installed on a motorized stage so that thermoreflectance change can be monitored. The spot size of the pump- beam is normally 50 μm and that of probe-beam is on the same order but smaller so that 1-dimensional assumption can be satisfied for the numerical analysis, which will be described later. The probe-beam reflected by the sample is converted to voltage signal in a photodetector connected to a lock-in amplifier, and the entire data collection procedure is performed on a computer using LabVIEW interface. Fig. 3 shows the photograph

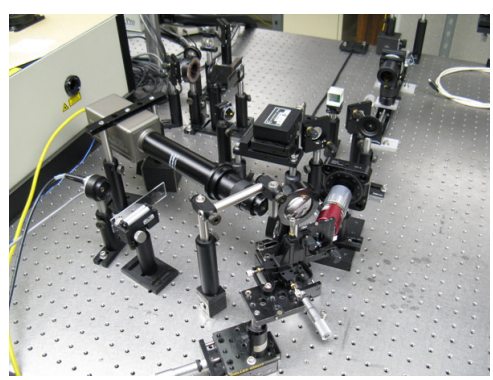

Fig. 3 A picture of the optical pump-probe setup in the Center for Quality Engineering & Failure Prevention at Northwestern University

of the actual setup in the Center for Quality Engineering & Failure Prevention at Northwestern University. Specific names of manufacturers and model numbers are provided in [9].

A typical response of thermoreflectance change from an aluminum(Al)-coated silicon(Si) substrate is presented in Fig. 4. When the optical path lengths(OPL) of the two beams are exactly the same, the probe-pulse monitors the reflectivity of surface at $t = 0$. Then the retroreflector on a stage is moved backward step by step to increase the delay time of the probe-beam, and in this way the decay of temperature-induced reflectivity changes afterwards are monitored. The resolution of plot depends on not only the pulse width of the ultrafast laser system, but also the movement resolution of the stage. The speed of light is 3×10^8 m/s, so displacement of retroreflector by 150 μm results in 1 ps delay on the time-domain plot. Once the plot is obtained, it is compared to a numerical model to extract thermal or mechanical properties from the best fit.

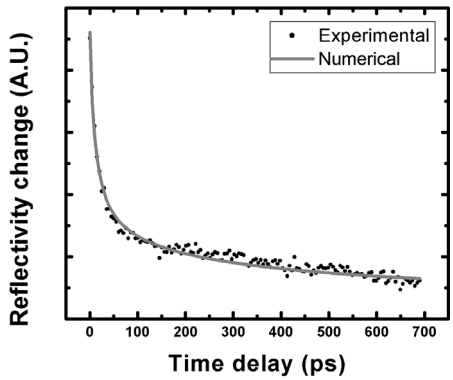

Fig. 4 The time-domain thermoreflectance change signal from an aluminum-coated silicon wafer

2.2 Numerical Analysis

In order to estimate the material properties, thermoelastic equations need to be solved. Depending on the time scale of heat-transfer process, it is divided into two regimes. The first one is the two-temperature model(TTM), which considers the absorption of optical energy by electrons and corresponding electron-phonon coupling during the first few picoseconds. The second one is the macroscopic Fourier heat conduction. While the TTM is useful in understanding ultrashort laser material processing and ballistic-diffusive heat transport phenomena, thermomechanical properties of thin-films and nanoscale materials can be extracted using the latter.

Suppose that the thermoreflectance of Al-coated Si is monitored as shown in Fig. 1. Following Richardson *et al.*[10], the partially coupled governing equations are as follows:

$$\kappa_{ij}T_{,ij} + W = \rho C_v \dot{T} \tag{1}$$

$$c_{ijkl}u_{l,kj} - B_{ij}T_{,j} = \rho \ddot{u}_i \tag{2}$$

where κ_{ij} is the thermal conductivity tensor, T is the temperature, ρ is the density of material, C_v is the specific heat, c_{ijkl} is the stiffness tensor, B_{ij} is the thermal-stress tensor, u_i is the displacement vector. W is the heating function determined by laser parameters:

$$W = \frac{\beta(1-R)}{2} e^{-\beta x} I(t) \tag{3}$$

where $\beta = 4\pi k_0/\lambda$ is the absorptivity (k_0 is the extinction coefficient and λ is the laser wavelength), $R = ((n_0\text{-}1)^2+k_0^2)/((n_0+1)^2+k_0^2)$ is the surface optical reflectance, n_0 is the refractive index of top layer material, and $I(t)$ describes the pulse shape:

$$I(t) = \begin{cases} I_0 \sin^2\left(\dfrac{\pi t}{\tau}\right), & 0 < t < \tau \\ 0, & t < 0,\ \tau < t \end{cases} \tag{4}$$

where τ is the pulse width. Boundary conditions are taken from the perfect contact between the film and substrate:

$$T^f\Big|_{x=d} = T^s\Big|_{x=d} \tag{5}$$

$$(\kappa_{ij}^f T_{,j}^f \cdot \hat{n})\Big|_{x=d} = (\kappa_{ij}^s T_{,j}^s \cdot \hat{n})\Big|_{x=d} \tag{6}$$

$$u^f\Big|_{x=d} = u^s\Big|_{x=d} \tag{7}$$

$$c_{ijkl}^f u_{k,l}^f\Big|_{x=d} = c_{ijkl}^s u_{k,l}^s\Big|_{x=d} \tag{8}$$

where the superscript f and s stands for 'film' and 'substrate'. d is the film thickness. Also, on the top surface of film there will not be heat flow and it is traction-free:

$$T_{,j}\Big|_{x=0} = 0 \tag{9}$$

$$\sigma_{ij}\Big|_{x=0} = [c_{ijkl}u_{k,l} - B_{ij}T]_{x=0} = 0 \tag{10}$$

Since the film is initially at rest, initial conditions are:

$$u\Big|_{t=0} = \dot{u}\Big|_{t=0} = T\Big|_{t=0} = \dot{T}\Big|_{t=0} = 0 \tag{11}$$

Since the spot size of pump-beam is much larger than that of the probe-beam, 1D assumption can be applied. Then the homogeneous and particular solutions can be obtained so that the temperature and displacement changes can be calculated. Finally, the optical reflectivity change of surface, ΔR, is determined as:

$$\frac{\Delta R}{R} = \frac{4(n_0^2 - k_0^2)[(n_0^2 - k_0^2 - p^2)I_\eta - 2n_0k_0J_\eta]v_\eta + 8n_0k_0I_\eta[2n_0k_0I_\eta + (n_0^2 - k_0^2 - p^2)J_\eta]w_\eta}{(n_0^2 - k_0^2 - p^2)^2/p - 4n_0^2 p} \tag{12}$$

where p = cosθ, and θ is the incident angle of probe-beam. v_η and w_η are the sensitivity coefficients of the complex dielectric constant, which determine the effect of the temperature (thermoreflectivity) or strain (piezoreflectivity) on the dielectric constant. I_η and J_η are given as follows:

$$I_\eta = K_0 \int_0^\infty A_\eta \exp(-2K_0k_0z)\sin(2K_0n_0z)dz \tag{13}$$

$$J_\eta = K_0 \int_0^\infty A_\eta \exp(-2K_0k_0z)\cos(2K_0n_0z)dz \tag{14}$$

where $A_\eta(z,t)$ is the temperature or the strain distribution. The solution can be numerically obtained using a finite-difference method(FDM) and material properties can be estimated from the best fit, as shown in Fig. 4. Similarly, materials of different structures, for example, trilayers composed of Al/sample material/ substrate or freestanding films, can be easily analyzed by increasing the number of layers in the governing equation and modifying boundary conditions.

3. Examples

Using the technique, materials in the form of 2D layers can be characterized. One of the most vigorously investigated materials is DLC thin-films and coatings. DLC is a class of material that comprises of distinct sp^2-to-sp^3 hybridization carbon(C) atoms and hydrogen content in the film. In general, the material becomes more diamond-like as the sp^3-bonded carbon content increases in the film. On the other hand, it becomes softer and less dense as the hydrogen(H) content increase, becoming graphite-like, as shown in Fig. 5[11]. DLC has many applications such as protective coatings for tribological tools[12], solid-lubricants for biomedical implants[13], chemical sensors[14], antireflection layers in photovoltaics[15], thermal actuators in MEMS devices[16], and so on.

DLC thin-films can be deposited using various techniques, such as plasma enhanced chemical vapor deposition(PECVD), graphite sputtering, laser ablation technique, filtered cathodic vacuum arcs, and so on[2]. Mechanical and thermal properties of DLC depends on the fabrication technique and specific deposition condition, researchers extensively characterized the material, especially using the picosecond ultrasonics.

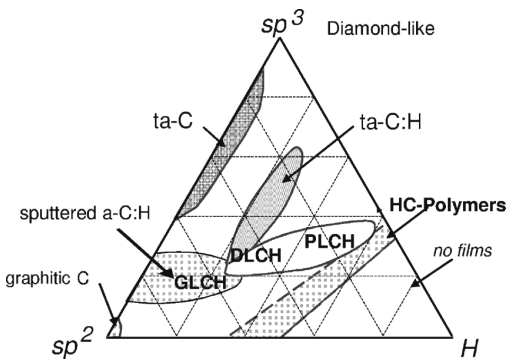

Fig. 5 Classification of DLC[10]

Morath *et al.*[17] shows thermal conductivity of DLCs and amorphous diamonds (*a*-D) fabricated from various techniques such as pulsed laser deposition, cathodic arc deposition, ion-beam sputter, plasma-assisted chemical vapor deposition, and direct ion-beam deposition in the range of $3\sim10^{-2}$ W/mK for DLC and $5\sim10^{-2}$ W/mK for *a*-D. Those values were larger than what the Einstein theory of heat conduction[18] predicts by factors of 3-5. According to the theory, heat transport in amorphous solids in the atomic scale is considered as a random walk of energy, rather than propagation of phonons:

$$\kappa_{CP}=\left(\frac{\pi}{6}\right)^{1/3}\kappa_B\left(\frac{N_A\rho}{M}\right)^{2/3}\sum_i c_i\left(\frac{T}{\theta_i}\right)^2\int_0^{\theta_i/T}\frac{x^3e^x}{(e^x-1)^2}dx \quad (15)$$

However, Morath *et al.* justified the disagreement that the thermal conductivity could be larger than that of a completely disordered material such as glass in the study by Cahill and Pohl[18] because of the long-range order in carbon materials.

Later, Arlene *et al.* [19] determined κ of PECVD-grown hydrogenated amorphous carbon (a-C:H) films grown at different temperatures (548~823 K). The value varied from 0.6 to 1.4 W/mK, and showed a general trend of increasing hardness and sound velocity with decreasing growth temperatures. Comparing the minimal thermal conductivity theory[18], their results showed good agreement within 20~30% deviation.

Kim *et al.* studied the effects of various growth conditions such as $H:CH_4$ flow-rate ratio for H-dilution[20], RF power[21], and deposition time[22] on the thermal diffusivity (α) of hydrogenated amorphous carbons deposited using the PECVD technique. Microstructural changes in the film were also characterized using optical transmission spectroscopy, Fourier transform infrared spectroscopy, and Raman spectroscopy so that their influence on α can be clarified. Strong dependence of the thermal property on the variation of sp^2 cluster size and sp^2 C content was observed, and the diffusivity values were similar or lower than those of *a*-C:H or *a*-D grown with similar deposition techniques.

As a closing remark, the ultrafast optical pump-probe method can be employed to the study of not only DLC but also other thin-film based novel materials and structures. Panzer *et al.* measured thermal properties of aligned single wall carbon nanotubes(SWNTs)[23]. In their experiment, an array of carbon nanotubes were grown on a silicon substrate coated with a layer of silicon dioxide(SiO_2), and the top surface was covered with 160-nm Al layer with a 20-nm palladium adhesion layer. The total thermal resistance of the structure was obtained to be 12 m^2 K MW^{-1}, and individual CNT-metal contact resistance was 10 m^2 K GW^{-1}. They anticipated that the total thermal resistance could be decreased below 1 m^2 K MW^{-1} by increasing the fraction of CNT-metal contacts. In the graphene research, Mak *et al.* evaluated the thermal interfacial thermal conductance (G_K) of mechanically exfoliated single and multilayer graphene on fused SiO_2 substrates[24]. G_K = 5000 W cm^2 K was obtained without any dependence of layer thickness, but it was comparable to those of carbon nanotubes in [25,26].

Conclusion

In this review paper, the principle and application of ultrafast optical pump-probe technique were introduced. Since the technique has very high temporal resolution appropriate for structures in micro and nanoscale, it has a lot of possibilities for investigations of thin-films in the area of micro/nano-NDE.

Acknowledgment

This work has partially been supported by the US National Science Foundation through award OISE-0730259.

References

[1] T. Murmu and S. C. Pradhan, "Small-scale effect on the vibration of nonuniform nanocantilever based on nonlocal elasticity theory," *Physica E,* Vol. 41, pp. 1451-1456 (2009)

[2] J. K. Luo, Y. Q. Fu, H. R. Le, J. A. Williams, S. M. Spearing and W. I. Milne, "Diamond and diamond-like carbon MEMS," *J. Micromech. Microeng.* Vol. 17, pp. S147-S163 (2007)

[3] O. Kraft, and C. A. Volkert, "Mechanical testing of thin films and small structures," *Adv. Eng. Mater.* Vol. 3, pp. 99-110 (2001)

[4] E. J. Gonzalez, J. E. Bonevich, G. R. Stafford, G. White and D. Josell, "Thermal transport through thin films: Mirage technique measurements on aluminum/ titanium multilayers," *J. Mater. Res.* Vol. 15, pp. 764-771 (2000)

[5] O. R. Shojaei and A. Karimi, "Comparison of mechanical properties of TiN thin films using nanoindentation and bulge test," *Thin Sol. Films* Vol. 332, pp. 202-208 (1998)

[6] D. G. Cahill, M. Katiyar and J. R. Abelson, "Thermal conductivity of a-Si:H thin films," *Phys. Rev.* B Vol. 50, pp. 6077-6081 (1994)

[7] G. A. Antonelli, B. Perrin, B. C. Daly, and D. G. Cahill, "Characterization of mechanical and thermal properties using ultrafast optical metrology," *MRS Bulletin*, Vol. 31, pp. 607-613 (2006)

[8] S. Krishnaswamy, "Photoacoustic methods of materials characterization," in Springer Handbook of Experimental Solid Mechanics, W. N. Sharpe, Ed., Springer, New York, USA (2008)

[9] Y. Y. Kim, H. A. Alwi, Q. Huang, R. Abd-Shukor, C. F. Tsai, H. Wang, K. W. Kim, D. G. Naugle and S. Krishnaswamy, "Thermal diffusivity measurement of $YBa_2Cu_3O_{7-x}$ thin film with a picosecond thermoreflectance technique," *Physica C*, Vol. 470, pp. 365-368 (2010)

[10] C. J. K. Richardson and J. B. Spicer, "Characterization of heat-treated tungsten thin films using picosecond duration thermoelastic transients," *Opt. Laser Eng*. Vol. 40, pp. 379-391 (2003)

[11] C. Casiraghi, A. C. Ferrari, and J. Robertson, "Raman spectroscopy of hydrogenated amorphous carbons," *Phys. Rev. B* Vol. 72, 085401 (2005)

[12] A. Erdemir and C. Donnet, "Tribology of diamond-like carbon films: recent progress and future prospects," *J. Phys. D: Appl. Phys.* Vol. 39 pp. R311-R327 (2006)

[13] G. Thorwarth, C. V. Falub, U. Müller, B. Weisse, C. Voisard, M. Tobler and R. Hauert, "Tribological behavior of DLC-coated articulating joint implants," *Acta Biomater*. Vol. 6, pp. 2335-2341 (2010)

[14] V. I. Polyakov, A. Yu. Mityagin, A. I. Rukovishnikov, B. Druz, I. Zaritsky and Y. Yervtukchov, "Effect of various adsorb-ates on electronic states of the thin diamond-like carbon films," *Diamond Relat. Mater.* Vol. 15, pp. 1926-1929 (2006)

[15] D. S. da Silva, A. D. S. Côrtes, M. H. Jr. Oliveira, E. F. Motta, G. A. Viana, P. R. Mei and F. C. Marques, "Application of amorphous carbon based materials as antireflective coatings on crystalline silicon solar cells," *J. Appl. Phys.* Vol. 110, 043510 (2011)

[16] J. K. Luo, J. H. He, Y. Q. Fu, A. J. Flewitt, S. M. Spearing, N. A. Fleck and W. I. Milne, "Fabrication and characterization of diamond-like carbon/Ni bimorph normally closed microcages," *J. Micromech. Microeng.* Vol. 15, pp. 1406-1413 (2005)

[17] C. J. Morath, H. J. Maris, J. J. Cuomo, D. L. Pappas, A. Grill, V. V. Patel, J. P. Doyle and K. L. Saenger, "Picosecond optical studies of amorphous diamond and diamondlike carbon: thermal conductivity and longitudinal sound velocity," *J. Appl. Phys.* Vol. 76, pp. 2636-2640 (1994)

[18] D. G. Cahill and R. O. Pohl, "Heat flow and lattice vibrations in glasses," *Solid State Commun.* Vol. 70, pp. 927-930 (1989)

[19] J. L. Arlein, S. E. M. Palaich, B. C. Daly, P. Subramonium and G. A. Antonelli, "Optical pump-probe measurements of sound velocity and thermal conductivity of hydrogenated amorphous carbon films," *J. Appl. Phys*. Vol. 104, 033508 (2008)

[20] Y. Y. Kim, H. A. Alwi, R. Awang and S. Krishnaswamy, "Photoacoustic measurements on thermal properties of hydrogenated amorphous carbon films: the effect of hydrogen dilution," *J. Phys.: Conf. Ser*. Vol. 278, 012006 (2010)

[21] Y. Y. Kim, H. A. Alwi, R. Awang and S. Krishnaswamy, "Influence of radio frequency power on thermal diffusivity of plasma enhanced chemical vapor deposition-grown hydrogenated amorphous carbon thin-films," *J. Appl. Phys*. Vol. 109, 113503 (2011)

[22] Y. Y. Kim, H. A. Alwi, R. Awang and S. Krishnaswamy, "Effects of deposition time duration on thermal diffusivity of hydrogenated amorphous carbon films," *Jpn. J. Appl. Phys*. Vol. 50, 125602 (2011)

[23] M. A. Panzer, G. Zhang, D. Mann, X. Hu, E. Pop, H. Dai and K. E. Goodson, "Thermal properties of metal-coated vertically aligned single-wall nanotube arrays," *J. Heat Transfer* Vol. 130, 052401 (2008)

[24] K. F. Mak, C. H. Lui and T. F. Heinz, "Measurement of the thermal conductance of the graphene/SiO_2 interface," *Appl. Phys. Lett*. Vol. 97, 221904 (2010)

[25] S. T. Huxtable, D. G. Cahill, S. Shenogin, L. P. Xue, R. Ozisik, P. Barone, M. Usrey, M. S. Strano, G. Siddons, M. Shim and P. Keblinski, "Interfacial heat flow in carbon nanotube suspensions," *Nature Mater*. Vol. 2, pp. 731-734 (2003)

[26] H. Maune, H. Y. Chiu and M. Bockrath, "Thermal resistance of the nanoscale constrictions between carbon nanotubes and solid substrates," *Appl. Phys. Lett*. Vol. 89, 013109 (2006)